OPEN

Enhancing Electrocatalytic Oxygen Reduction on Nitrogen-Doped Graphene by Active Sites Implantation

Leiyu Feng, Lanqin Yang, Zujing Huang, Jingyang Luo, Mu Li, Dongbo Wang & Yinguang Chen

State Key Laboratory of Pollution Control and Resources Reuse, School of Environmental Science and Engineering, Tongji University, Shanghai 200092, People's Republic of China.

The shortage of nitrogen active sites and relatively low nitrogen content result in unsatisfying eletrocatalytic activity and durability of nitrogen-doped graphene (NG) for oxygen reduction reaction (ORR). Here we report a novel approach to substantially enhance electrocatalytic oxygen reduction on NG electrode by the implantation of nitrogen active sites with mesoporous graphitic carbon nitride (mpg-C_3N_4). Electrochemical characterization revealed that in neutral electrolyte the resulting NG (I-NG) exhibited super electrocatalytic activity (completely 100% of four-electron ORR pathway) and durability (nearly no activity change after 100000 potential cyclings). When I-NG was used as cathode catalyst in microbial fuel cells (MFCs), power density and its drop percentage were also much better than the NG and Pt/C ones, demonstrating that the current I-NG was a perfect alternative to Pt/C and offered a new potential for constructing high-performance and less expensive cathode which is crucial for large-scale application of MFC technology.

F uel cells (FCs) offer a great opportunity to obtain cleaner and more sustainable energy in the 21st century. One of the great challenges encountered in fuel cell technology is to explore innovative, alternative and non-precious metal cathode catalysts with low cost, high activity and practical durability for oxygen reduction reaction (ORR) in the long-term run because the current platinum (Pt) or its alloys suffer from high cost, low-reverses in nature, and formation of PtO layer at the Pt surface[1,2], although they have been demonstrated to be the best electrode materials for ORR. Thus, the development of cost-effective and durable catalysts for efficient oxygen reduction to reduce or even replace Pt has becoming one of the most attractive topics in fuel cell field.

Recently, as one kind of the reasonable alternatives to Pt catalysts, non-precious metal-free carbon materials have been revealed to be viable given their comparable catalytic activities toward ORR[3–6]. Among these carbon materials, nitrogen-doped graphene (NG) has drawn the most attention and been accepted as an excellent substitute for Pt to improve the commercialization prospect of fuel cell technology[7–10]. Generally, nitrogen doping can enhance the electrical property of carbon matrix of graphene, resulting in an improvement of cross correlation between carbon and guest molecules[7–10]. However, the shortage of nitrogen active sites and low nitrogen content (lower than 5%) always result in unsatisfying eletrocatalytic activity and durability of NG for ORR. The development of NG materials with more nitrogen active sites and relatively higher nitrogen content is therefore highly desirable.

As is well known, graphitic carbon nitride (g-C_3N_4), which can be synthesized from a simple precursor, has been reported to show remarkably high catalytic activities for lots of chemical reactions, such as photocatalytic hydrogen production and contaminant degradation due to its abundant nitrogen active sites[11]. If active sites from g-C_3N_4 could be implanted to the nanosheets of NG, the electrocatalytic activity and durability of NG for ORR would be enhanced due to a bountiful supply of active sites which have been considered to be related to electron-rich N atoms with electron lone pairs and electrondonating conjugated π-bond systems[12]. Also, the electrocatalytic activity of implanted g-C_3N_4 itself for ORR could be improved by NG with super conductivity, because it has been documented that one of the effective strategies to improve the ORR activity of non-conductive g-C_3N_4 is the application of conductive carbon support to reduce the electron accumulation on the surface of catalyst[13–15]. The synergistic coupling interactions between NG and g-C_3N_4 would drive NG to possess better electrocatalytic activity and durability for ORR than the pristine one. Till now, however, reports on the enhancement of ORR activity and durability of NG by the implantation of nitrogen active sites are rare[16], and no related practical electrochemical applications have been done.
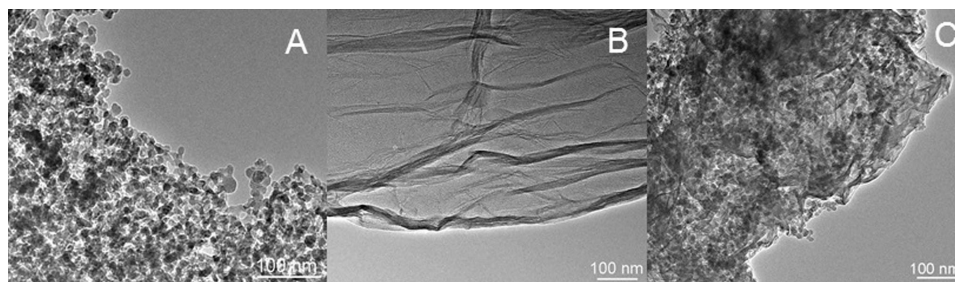
Figure 1 | TEM analysis of (A) mpg-C_3N_4, (B) NG and (C) I-NG.

Herein we reported the implantation of nitrogen active sites to NG nanosheets (named as I-NG) with mesoporous g-C_3N_4 (mpg-C_3N_4) which has been demonstrated to have a larger number of nitrogen active sites present on its surface than other types of g-C_3N_4[11]. The synthesized I-NG material showed amazing electrocatalytic activity (100% of four-electron pathway) and durability (nearly no activity change after 100000 potential cyclings) for ORR, and remarkable metabolite tolerance to crossover effects in neutral phosphate buffer solution (PBS). Recently, extensive investigations have been performed on microbial fuel cells (MFCs), which can be applied to the conversion of biomass into electricity and the treatment of wastewater, whereas their large-scale applications are hampered by the lack of cheap organics-resistant ORR catalysts[17]. Researcher has attempted to use NG as ORR catalyst in MFCs, but the performance of power output is still needed to be improved due to the unsatisfying ORR activity of NG[8]. When I-NG was used as cathode catalyst in MFCs of current study, we found that the outcome of power generation was exciting with an obvious promotion compared with those obtained in MFCs with pristine NG, even Pt/C, offering a new potential for constructing a large-scale MFC device with high-performance and less expensive cathode.

Results

Implantation of active sites to NG. Typically, the implantation of nitrogen active sites to NG was completed by two-step process (Schematic diagram is shown in Figure S1). In the first step, NG and mpg-C_3N_4 were prepared respectively by one-pot solvothermal and self-condensation reactions. In the second step, mpg-C_3N_4 with abundant nitrogen active sites was implanted to NG nanosheets *via* sonochemical approach. Details on the implantation of nitrogen active sites (with only about 5.0 wt% mpg-C_3N_4) can be found in the section of Materials Synthesis.

Morphology and structure characterization. The morphologies and structures of synthesized materials were investigated respectively by scanning electron microscopy (SEM) (Figure S2) and transmission electron micros-copy (TEM) (Figure 1). Figure S2A demonstrates that the as-prepared mpg-C_3N_4 was composed of particles with high uniform dispersion, small size and porous mpg-CN surface. The TEM images of mpg-C_3N_4 (Figure 1A) shows the presence of a disordered but well-developed pore system of spherical mesopores within mpg-C_3N_4, and a pore diameter close to 12 nm directly reflecting the size of silica template. As shown in Figure 1B and S2B, the synthesized NG displays two-dimensional sheets with chiffon-like ripples and wrinkles, which can induce the pores on the surface of NG making itself possess a large surface area. From the SEM and TEM images of I-NG (Figure 1C and S2C), both mentioned morphologies and structures can be seen clearly, revealing that mpg-C_3N_4 particles have been implanted successfully to the synthesized NG.

Raman spectroscopy is the most direct and nondestructive method to characterize the structure and quality of carbon materials, particularly to determine the layers of graphene. In the Raman spectrum of I-NG within the range of 500–3500 cm^{-1} there were three distinguished peaks at 1328, 1586 and 2650 cm^{-1}, representing respectively for D, G and 2D band (Figure 2A). Usually, in the spectra of nitrogen-doped carbon materials the D band corresponds to disordered sp^2 microdomains introduced by the linking with N atoms, and G band to the symmetric E$_{2g}$ vibrational mode of sp^2 carbon domains in the graphite-like structures. In the present study, the peak intensity ratio of D to G band (I_D/I_G) was calculated to be about 0.12, suggesting that the I-NG material remained at a high crystalline quality. The 2D peak is the most prominent feature of graphene in the Raman spectrum, and its position and shape are sensitive to the layer number. In the current investigation, both of synthesized I-NG
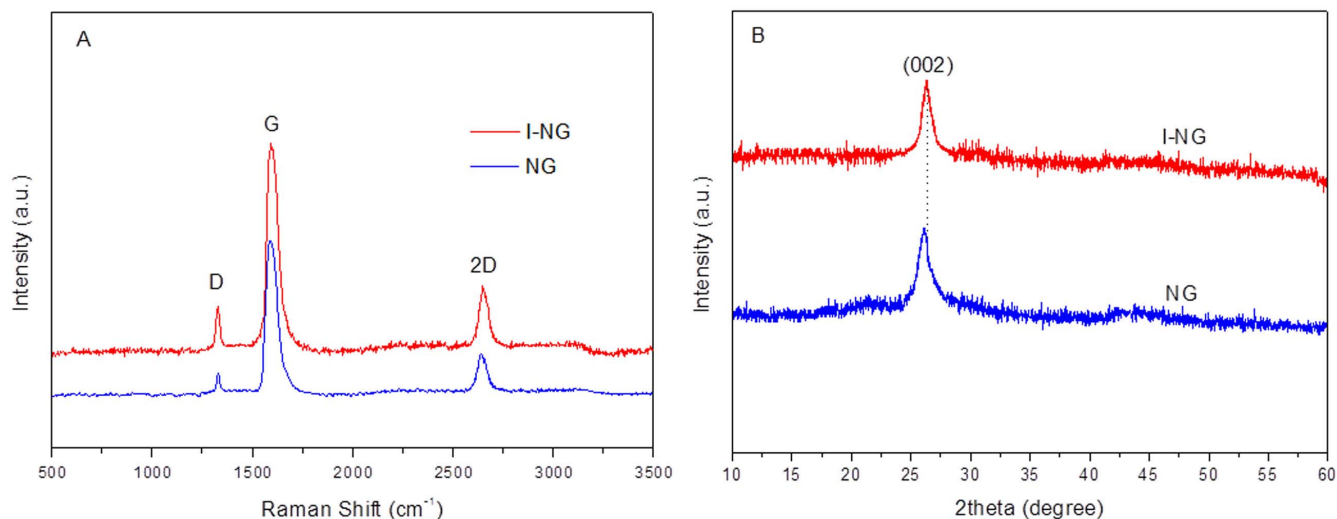

Figure 2 | (A) Raman spectra and (B) XRD patterns of I-NG and NG.

and NG exhibited broad and up-shifted 2D peaks in the Raman spectra, which indicated that the synthesis process used in this study resulted in the few-layer NG. Moreover, it is noted that the position and shape in the Raman spectrum of I-NG were similar with that of NG, suggesting that the structure of NG remain stable during the implantation of nitrogen active sites. The X-ray diffraction (XRD) patterns of the synthesized I-NG and NG are presented in Figure 2B. It was observed that the NG sample exhibited an intensive peak centered at 26.1° which evidenced its high crystalline quality, showing good conformity with that of NG synthesized in the previous publication[8]. When nitrogen active sites were implanted into NG nanosheets, the I-NG kept the XRD peak at 26.3°. Obviously, the XRD peak positions of I-NG changed little compared with those of NG, further demonstrating that the crystalline quality of I-NG material remained satisfying in despite of the implantation of nitrogen active sites.

X-ray photoelectron spectroscopy (XPS) measurements were performed to probe the chemical composition and the content of nitrogen in the I-NG material (Figure 3). The survey scan spectrum from XPS analysis for I-NG revealed the presence of C1s, O1s and N1s without any other impurities, demonstrating that the current I-NG material was completely metal-free. In the spectrum of I-NG, the peaks at 288.9, 399.2, and 535.0 eV corresponded to C1s of sp2 C, N1s, and O1s of the absorbed oxygen, respectively (Figure 3A). The atomic ratio of nitrogen to carbon (N/C) in the synthesized I-NG was calculated to be about 19.7% from the peak areas of C1s and N1s and

their atomic sensitivity factors whereas that of the pristine NG was only 11.9%. Thus, the atomic ratio of N/C in the current I-NG was significantly enhanced by the implantation of active sites. Generally, the reported atomic ratio of N/C in NG with good electrocatalytic activity was only around 4%[18–20]. As the carbon nanomaterials with higher atomic ratios of N/C have been documented to exhibit much better physiochemical properties, such as electrocatalytic activity, electrical conductivity, etc.[21,22], the I-NG prepared in the present study might have a wider range of practical application.

The detailed C 1s spectrum of I-NG ranging from 280 to 296 eV is shown in Figure 3B. It can be found that there were four different C groups in XPS spectrum of I-NG, which were characterized by the appearance of several spectral peaks: original C-C at 285.5 eV, C-OH at 286.4 eV in NG, C-N-C at 287.3 eV in mpg-C_3N_4, and a new C=O at 289.0 eV in I-NG, respectively. The high resolution XPS N 1s spectrum of I-NG is shown in Figure 3C, and can be deconvoluted into three different signals with binding energies of 398.9, 400.1 and 401.4 eV which corresponded to pyridinic N (N1), pyrrolic N (N2) and graphitic N (N3), respectively. Further exploration found that the content of pyridinic N in I-NG nanosheets was greatly improved by the implantation of active sites (The high resolution N 1s spectrum of pristine NG is shown in Figure 3D). Besides those of C1s and N1s, O1s peak at 535.8 eV was also observed in the XPS spectrum of synthesized I-NG. The presence of O1s could be attributed to the moisture, atmospheric O_2, or CO_2 adsorbed on I-NG nanosheets as well as the residual oxygen-containing groups, such
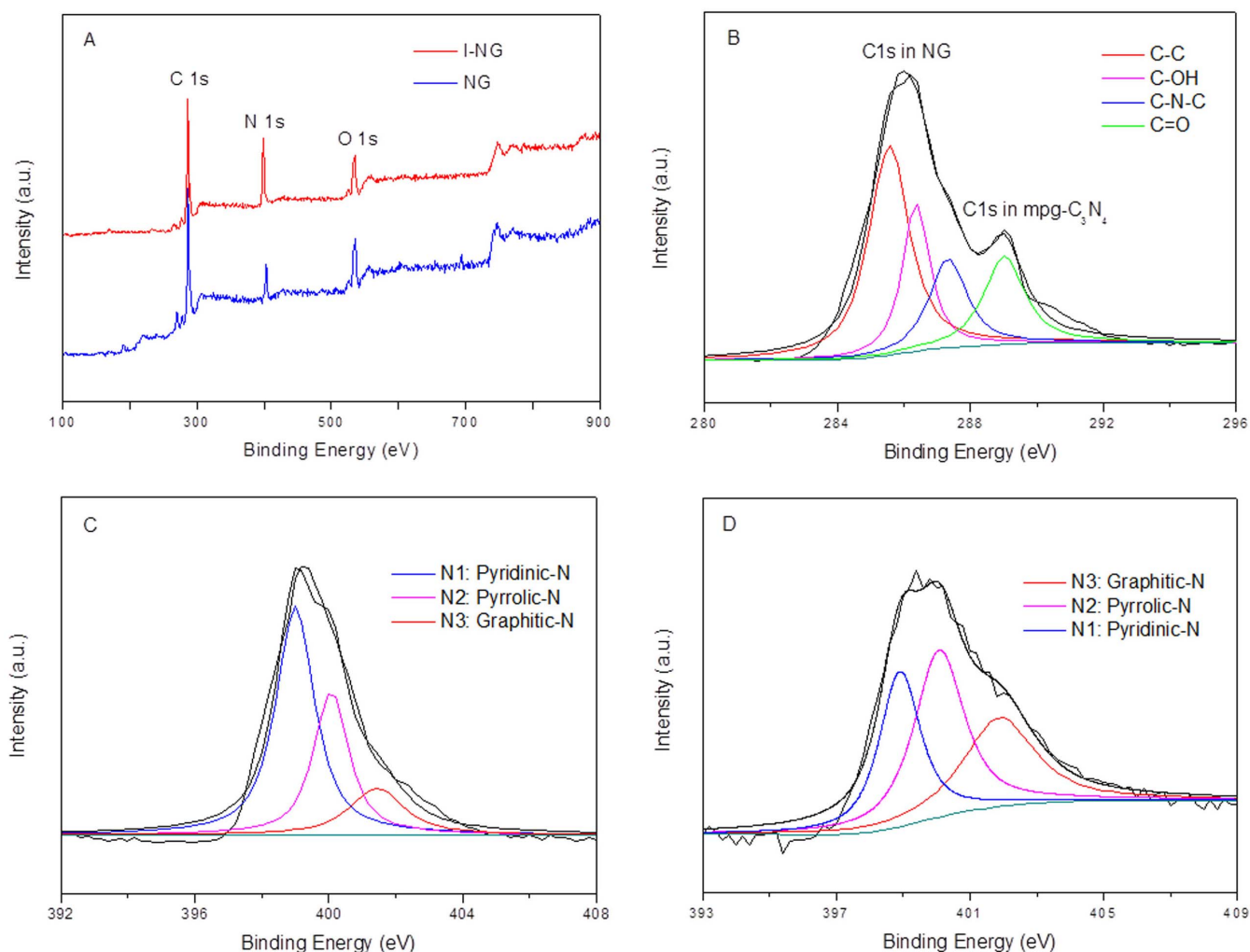

Figure 3 | (A) XPS survey for I-NG and NG, (B) high-resolution C 1s of I-NG, (C) N 1s spectrum of I-NG and (D) N 1s spectrum of NG.

as carbonyl and carboxyl groups, that remained at the edges or in the plane of graphene. It has been reported previously that a high content of oxygen in carbon nanomaterials can lead to a strong ability for O_2 adsorption[23], which might be another advantage for I-NG when being used as the eletrocatalyst for oxygen reduction.

Evaluation of electrocatalytic activity and durability. The electrocatalytic activity of I-NG for ORR was first characterized by cyclic voltammetry (CV) in O_2-saturated 50 mM PBS (pH 7.0), which is commonly used in biological systems, on a glassy carbon electrode and compared with several other catalysts (Figure 4A). As shown in Figure 4A, there was a negligible ORR peak at relatively lower cathode voltage on the CV curves of mpg-C_3N_4, corresponding to the poor electrocatalytic activity for ORR caused by the poor electron transfer ability derived from its nonconductive nature[11]. Similar with the previous study[8], the as-prepared NG showed a clear ORR peak comparable with that of Pt/C, indicating that the NG synthesized in this study had an excellent electrocatalytic activity for ORR in neutral PBS. When the NG was implanted with plenty of nitrogen active sites, the I-NG electrode displayed a much more obvious ORR peak with a larger cathode current compared with those of NG and Pt/C, demonstrating a better electrocatalytic performance for ORR. Similar trends in the ORR activities were

observed based on a series of linear sweep voltammograms (LSV) on a rotating disk electrode (RDE) (Figure 4B). The more positive onset potential and higher ORR current density on I-NG than mpg-C_3N_4, NG and Pt/C electrodes occurred.

It is well known that ORR is a rather complex multistep process and the electrocatalytic performance of cathode catalyst depends on the route of ORR. The rotating ring-disk electrode (RRDE) measurements were performed to further investigate the ORR pathways catalyzed by I-NG under the steady-state conditions in neutral PBS. Figure 4C shows the ring and disk currents recorded at 1200 rpm in PBS for I-NG, NG, mpg-C_3N_4 and Pt/C. Obviously, the I-NG sample exhibited a much higher disk current, and a nearly negligible ring current (Figure S3). The transferred electron number ($n = 4I_D/(I_D + I_R/N)$, where I_D is the faradic disk current, I_R is the faradic ring current, and N = 0.47 is the collection efficiency determined with $Fe(CN)_6^{3-/4-}$ as probe) per oxygen molecule involved in the ORR process was calculated to be 4.0 for I-NG at the potential of −0.10 V, indicating that the reduction process of I-NG was a complete four-electron pathway. The transferred electron numbers per oxygen molecule for NG, mpg-C_3N_4 and Pt/C were respectively 3.7, 2.1 and 3.9. Obviously, the electrocatalytic activity of NG was significantly enhanced by the implantation of active sites.
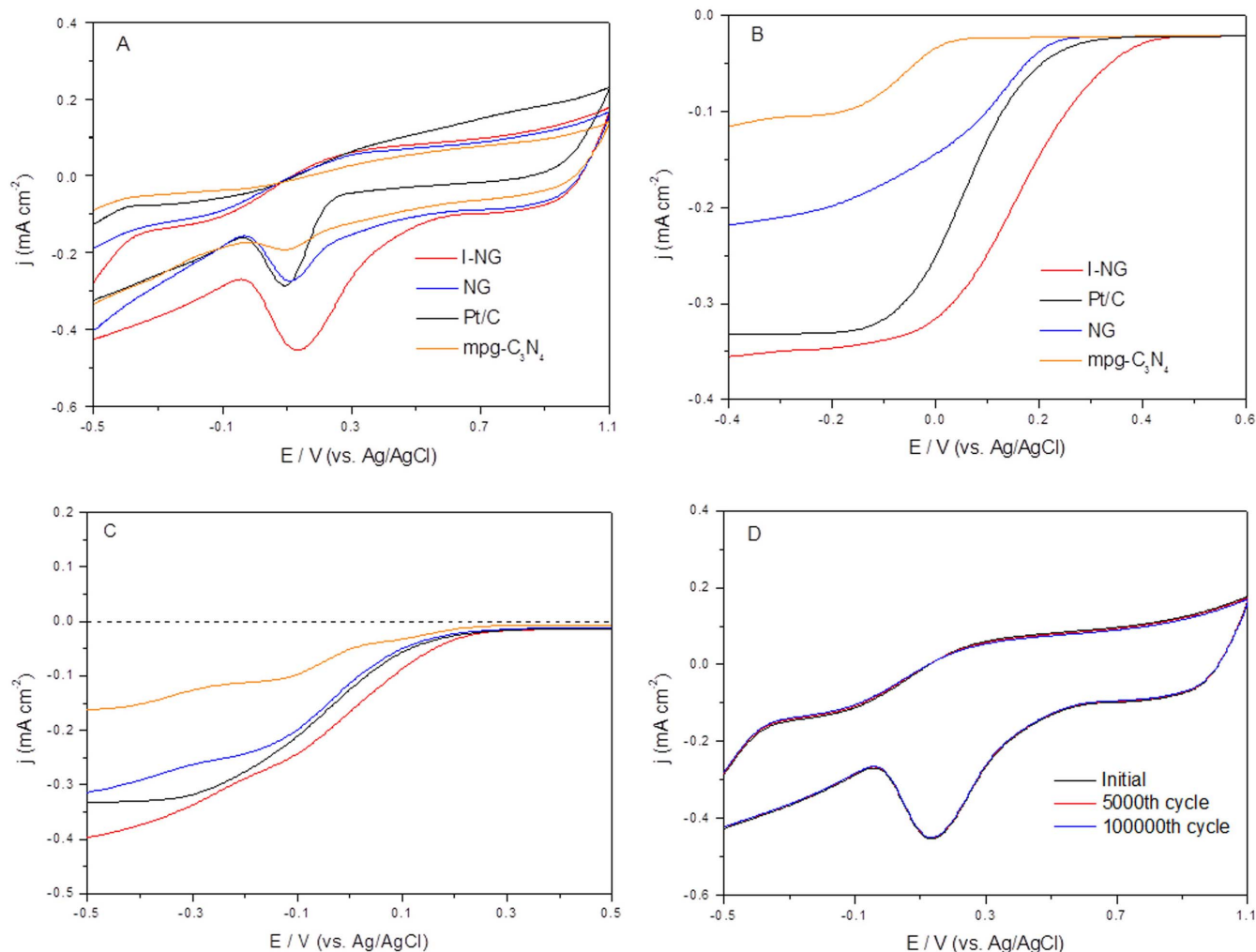

Figure 4 | Electrochemical evaluation. (A) Cyclic voltammograms (CVs) of ORR on various Electrocatalysts at the scan rate of 0.1 V s^{-1}. (B) LSV of various electrocatalysts on RDE at 1200 revolutions per minute (rpm). (C) RRDE disk currents of I-NG (red line), Pt/C (black line), NG (blue line) and mpg-C_3N_4 (orange line) electrodes at a rotation rate of 1200 rpm. The Pt ring electrode was poised at 0.5 V. (D) CVs of ORR on I-NG before and after a continuous potentiodynamic swept for 5000 and 100000 cycles at room temperature ($25 \pm 1°C$). The electrolyte used during voltammogram measurements was the O_2-saturated 50 mM PBS solution (pH 7.0).

The durability of I-NG was evaluated by the chronoamperometric response under the constant cathode voltage. As shown in Figure 4D, the newly developed catalyst exhibited high durability with a negligible attenuation after 5000 and 100000 continuous potential cyclings. Also as seen in Figure S4, there is no visible morphology change for I-NG after durability test, suggesting that the synthesized I-NG is a class of stable catalysts for ORR.

The metabolite tolerance ability is an important feature of catalysts when being used to catalyze the ORR in biological systems, and also an obvious disadvantage of Pt-based catalysts. In the present study, the crossover behavior (metabolite tolerance ability) of synthesized I-NG was investigated by the addition of 5 mM sodium formate (Figure S5). It is clearly visible that the cathode ORR current remained largely unchanged after sodium formate addition into the electrolyte solution, which demonstrated that the I-NG material possessed remarkably good tolerance to the metabolite crossover effect. The as-prepared I-NG might therefore be an ideal electrocatalyst with high metabolite tolerance ability when being used in biological systems although the related examination of tolerance ability for other metabolites, such as methanol, sulphide, etc., is still needed to be performed.

Application of I-NG as cathode catalyst in MFCs. Various oxidants have been used as electron acceptors at the cathode of MFCs, whereas the most sustainable electron acceptor is oxygen due to its easy availability in the environment with the capacity to give a high power output[24,25]. Thus, in this study the performance of power output in MFCs with I-NG as cathode catalyst (shorten as I-NG-MFCs, Figure S6) was evaluated, and MFCs with NG (NG-MFCs) and Pt/C (Pt/C-MFCs) were set as the comparisons (Figure 5). The obtained polarization curves and power densities are presented in Figure 5A. It was observed that based on the polarization data the maximum power density in I-NG-MFCs was 1618 ± 50 mW m^{-2}, whereas in NG-MFCs and Pt/C-MFCs it was 1350 ± 30 and 1423 ± 25 mWm^{-2}, which were $16.6 \pm 1.2\%$ and $12.1 \pm 1.5\%$ lower than that in I-NG-MFCs (Figure 5A). The MFCs with I-NG as cathode catalyst had much better capacity of power generation.

It is well known that cathode catalyst with an excellent durability is one of the important needs during the development of MFC technology. The durability of current I-NG in MFCs was therefore examined by evaluating the effect of operation time on the maximum power density, and those of NG and Pt/C were set as the references. It can be seen from Figure 5B that with operation time of about 80 d the decrease of maximum power density in I-NG-MFCs was only $4.8 \pm 0.3\%$, whereas it was $9.1 \pm 0.6\%$ and $16.0 \pm 0.9\%$ in NG-MFCs and

Pt/C-MFCs. The I-NG-MFCs had a much better stability for power output.

Discussion

In the present study nitrogen active sites was implanted successfully to NG nanosheets, forming a new ideal electrocatalyst for ORR in neutral electrolyte. The approach for the synthesis of current I-NG material was easy-to-operate and catalyst-free using low-cost industrial reagents. Thus, the price of I-NG would be expected to be much lower than those of Pt or its alloys without regard to labor cost, which was crucial when the current material was used as cathode catalyst in fuel cell systems.

During the implantation of active sites, the morphologies of both NG and mpg-C_3N_4 remained unchangeable (Figure 1 and S2), and their crystalline qualities were demonstrated to remained high based the analysis of Raman and XRD. From the XPS spectrum of I-NG, it can further been seen that there were no other impurity peaks except those of C1s, O1s and N1s, which suggested that the synthesized catalyst was completely metal-free. During the preparation of I-NG, the implantation of mpg-C_3N_4 not only improved the nitrogen content from 11.9% for NG to 19.7% for I-NG, but also brought large amounts of pyridinic N, for NG nanosheets. Usually, in the nanosheets of nitrogen-doped carbon materials the nitrogen active sites correspond to pyridinic[4,7,8,26,27] or graphitic N[28]. It has been documented that N-graphene prepared using a chemical vapor deposition (CVD) method showed a high electrocatalytic activity toward ORR with a limiting current density three times larger than 20 wt% Pt/C due to the pyridinic N-abundant structure[8]. However, Lai et al reported that the electrocatalytic activity of NG was dependent on the graphitic N content which determined the limiting current density, while the pyridinic N content improved the onset potential for ORR[28]. Although which type of N is the most catalytically active site for ORR is still highly controversial, the I-NG material with more nitrogen active sites would be expected to have the stronger ability of weakening the O-O bond *via* the bonding between the oxygen and nitrogen and/or the adjacent carbon atom, and facilitate the reduction of O_2. It is worth to note that the proportion of pyrrolic N in the synthesized I-NG was reduced by active sites implantation, also giving benefits for the enhancement of electrocatalytic activity because pyrrolic N are always chemically active themselves[28].

In the following electrochemical measurements, it is demonstrated that the electrocatalytic activity, even durability for ORR on I-NG electrode was truly enhanced by the implantation of mpg-C_3N_4. Compared with Pt/C, NG and mpg-C_3N_4, the I-NG electrode revealed a more obvious ORR peak with a larger cathodic current,
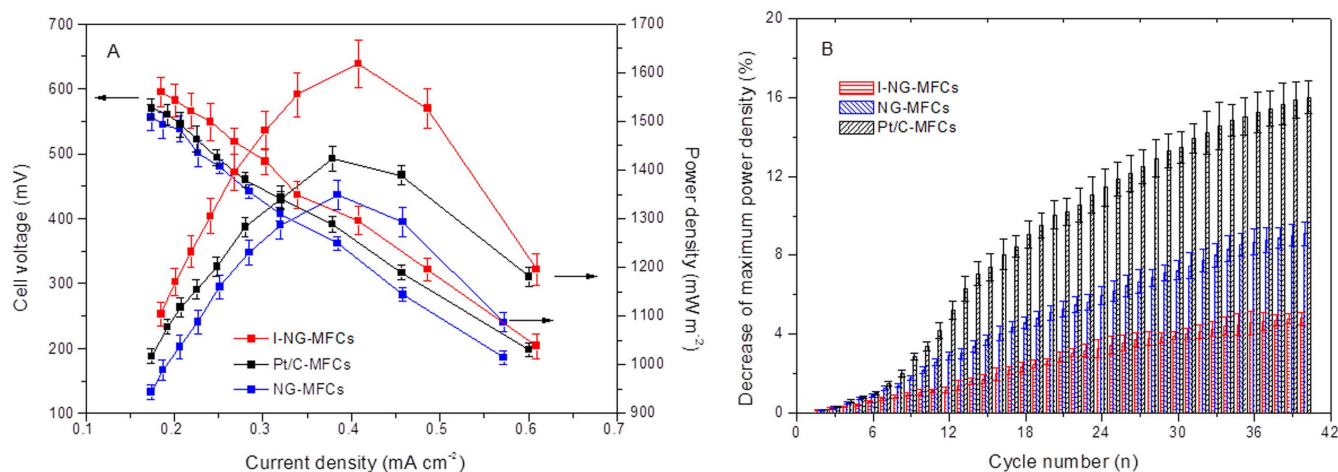

Figure 5 | (A) Power densities and cell voltages in I-NG-MFCs, NG-MFCs and Pt/C-MFCs. (B) Decrease of maximum power density with cycle number at an external resistance of 1000 Ω. 40 cycles represent about 80 days. Error bars represent standard deviations of duplicate tests.

indicating a better electrocatalytic performance for ORR. LSV further revealed the more positive onset potential and higher ORR current density, consistent with the CV observations. Besides, the wide current plateau on I-NG electrode was considered as the strong limiting diffusion current, indicating a diffusion-controlled process related to an efficient four-electron dominated ORR pathway. To quantify the ORR electron transfer pathway, the RRDE technique was employed, and only one-step process for ORR was observed for I-NG, suggesting a complete four-electron pathway for ORR, which was confirmed by the corresponding current for HO_2^- oxidation recorded at the Pt ring electrode. As can be seen in Figure S3, the amount of HO_2^- generated on the I-NG electrode was significantly less than that on mpg-C_3N_4, even NG and Pt/C, indicating that I-NG was a more efficient ORR electrocatalyst. Combining the above results with those of XPS analysis, we can conclude that in the current I-NG the pyridinic N was the most catalytically active site for ORR, in accordance with the studies of Kundu et al.[26] and Rao et al.[27], and the implantation of nitrogen active sites resulted in the remarkable improvement of electrocatalytic activity and durability. To our best knowledge, the electrocatalytic activity and durability of metal-free I-NG for ORR in the neutral electrolyte was better than any other CN materials reported previously, even better than those of Pt or its alloys.

It is well known that almost all the reported electrocatalysts with superior activity and durability as alternatives of Pt catalyst are the metal-based materials, and the metal-free materials with such an ideal electrocatalytic activity and durability for ORR were rather scare[29–31]. The related reasons could be explained as follows. The most important one was that mpg-C_3N_4 provided sufficient nitrogen content, especially nitrogen active sites, for NG nanosheets, which drove the I-NG material to have the strong ability of weakening the O-O bond *via* the bonding between the oxygen and nitrogen and/or the adjacent carbon atom as a feasible metal-free electrocatalyst. The other one was that the electron transfer efficiency of mpg-C_3N_4 itself was significantly improved by using NG as the conductive support, which in turn facilitated the performance of NG. The obvious synergistic interactions between NG and mpg-C_3N_4 brought I-NG super eletrocatalytic activity and durability for ORR (Schematic diagrams were summarized in Figure 6).

We further studied the electrocatalytic performance of current I-NG when being used as cathode catalyst in a real biological system (MFCs), and both the capacity and durability of power output in I-NG -MFCs were found much better than those in MFCs with NG and Pt/C as cathode catalyst. In the present study the internal resistances of I-NG-MFCs and Pt/C-MFCs based on EIS analysis were determined to be 75 ± 4 and 88 ± 5 Ω, respectively. It is well known that the internal resistance of a MFC reactor mainly consists of the electrode ohmic loss caused by the movement of electrons through the electrode and wires. MFC reactors used in this study had the same configuration, such as anode material, electrode distance, wires, *etc.* Thus, the difference of internal resistance between MFC reactors derived from the difference of the electrical characteristics, especially the conductivity, between the synthesized I-NG and Pt/C. In the current investigation the measured electrical conductivities of I-NG and Pt/C cathodes were 66 ± 2 and 45 ± 2 S cm^{-1}, respectively. Clearly, the higher conductivity of I-NG cathode resulted in the lower internal resistance of I-NG-MFCs, further benefiting the capacity of power generation. In this study, the maximum power density over operation time in MFCs was found to drop more or less. It has been proposed in the literature that the drop of maximum power density in MFCs was attributed to the proton limitation caused by biofilm formation on the cathode and activity deterioration of electrocatalyst[32]. Here, the thickness of biofilms on the cathodes of I-NG-MFCs, NG-MFCs and Pt/C-MFCs was measured to be about 0.1 cm with operation time of about 80 d, which seemed to be one of the reasons for the decrease of maximum power density. However, it is worth noticing that the decrease of maximum power density in MFCs without cathode catalyst, which was caused by proton limitation only, was 1.0 ± 0.2% (detailed data not shown here), revealing that the activity deterioration of cathode catalyst was the main reason for the decrease of maximum power density in I-NG-MFCs, NG-MFCs and Pt/C-MFCs. Thus, the synthesized I-NG material also had the satisfying electrocatalytic durability in MFCs when being used as cathode catalyst for a long run.

In the previous investigations many efforts have been given to develop alternative catalyst, such as carbon fiber[33], graphite[34], transition metal porphyrines and phthalocyanine[32,35], to replace or reduce the content of Pt in MFCs. As far as we know, however, the performance of power generation was always unsatisfying compared with that with Pt/C when those so-called alternative catalysts were applied in MFCs. The I-NG-MFCs have been proved to have the excellent capacity and durability of power generation, even better than Pt/C-MFCs. The novel I-NG catalyst, therefore, might be an ideal candidate for the alternative of Pt catalyst in MFCs, offering a new potential for constructing high-performance and less expensive cathode that is crucial for the large-scale practical application of MFC and other biological technology.

In summary, we have established a facile strategy for the enhancement of ORR activity and durability of NG nanosheets by the implantation of nitrogen active sites, and the synthesized I-NG material were demonstrated to possess super electrocatalytic activity and durability for ORR in the neutral electrolyte, and could be further used as a perfect alternative of Pt catalyst in MFCs for efficient and durable electricity generation. Arising from the success implantation of nitrogen active sites to NG nanosheets, the obtained I-NG might benefit not only fuel cell systems, but also lithium ion batteries (LIBs). The application of I-NG with a high pyridinic N content as a potential anode material could drive LIBs to achieve a high reversible capacity at a high charge/discharge rate as the pyridinic N plays an effective role in lithium intercalation and deintercalation[36].

Methods

Materials synthesis. All reagents purchased from Sinopharm Chemical Reagent Co. Ltd. (China) were of analytical grade and used without further purification. All the solutions were prepared with doubly distilled water.

Graphite oxide (GO) was prepared from graphite powder by a modified Hummers method[37,38]. In a typical reaction, 2.0 g of graphite, 1.0 g of sodium nitrate, and 50 mL of concentrated sulfuric acid were stirred together in an ice bath for 24 h. Under vigorous agitation, 6 g of potassium permanganate was slowly added. As the mixing was completed, the solution was transferred to a 40°C water bath for 30 min. Next, 100 mL of distilled water was gradually added, and the solution was stirred for 15 min while the temperature was increased to 90 ± 5°C. Finally, the solution was diluted with 300 mL of distilled water and treated with 10 mL of H_2O_2 (30%), turning the color from dark brown to yellow. The warm solution was then filtered and washed with 5% HCl solution and sequentially washed with distilled water. The resultant solid was finally dried under vacuum at 70°C overnight.

Nitrogen-doped graphene (NG) was synthesized by a one-pot solvothermal process. In a typical procedure, 100 mg of GO was added in 10 mL of water to give a dark brown solution and sonicated for 1 h. Sequentially, 60 mL of ammonia solution (25–28 wt% in water) was added, and the mixture was transferred into a Teflon-lined autoclave with volume of 180 mL and heated at 220°C for 12 h. The synthesized NG was collected by centrifugation and desiccation at 60°C overnight in a vacuum to remove the physisorbed NH_3.

The mesoporous graphitic carbon nitride (mpg-C_3N_4) material was prepared according to the method described by Goettmann[39]. Typically, 10 g of cyanamide was melted in 10 mL of H_2O, followed by dropping a certain amount of a 40% dispersion of 12 nm SiO_2 particles in water (Ludox HS40). The mixtures were then stirred at 70°C to remove the water. The dry solid was subjected to sinter about 2 h to reach temperature of 550°C and then to 600°C for 10 h under static vacuum in a sealed quartz ampoule. The resulting powder was treated with NH_4HF_2 solution (4 M) for 24 h to remove the silica template. The powders were then centrifuged and washed three times with distilled water and twice with ethanol. Finally, the mpg-C_3N_4 powers were dried at 70°C under vacuum overnight.

The implantation of nitrogen active sites into NG nanosheets was completed *via* sonochemical approach. The typical procedure was as follows: 100 mg of NG was dispersed in 100 mL of concentrated HNO_3 (70%) at 50°C to induce hydrophilicity. Then, a certain amount of mpg-C_3N_4 powder was added into the above solution. The suspension was ultrasonicated for 10 h and then dried at 80°C under vacuum for
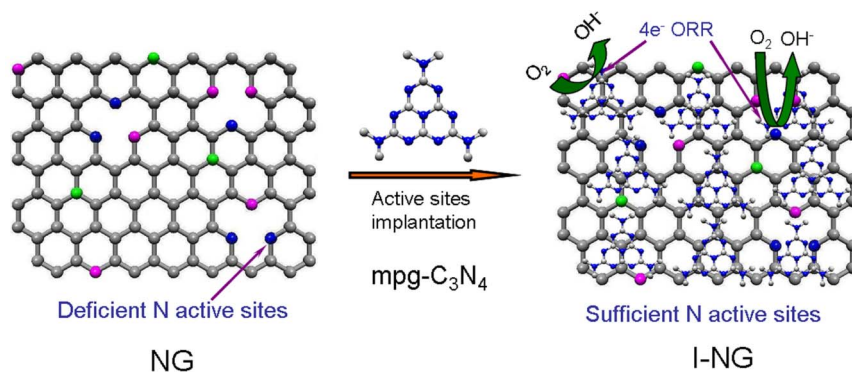
Figure 6 | Schematic diagrams of synergistic interactions between NG and mpg-C₃N₄.

12 h. With this method the I-NG material (with about 95.0 wt% NG and 5.0 wt% mpg-C₃N₄) was obtained.

Characterization of the synthesized materials. Transmission electron microscopy (TEM) images for the synthesized catalysts were recorded on a Philips EM-430 TEM unit, and scanning electron microscopy (SEM) ones on a Hitachi S-4800. Raman microspectroscopy was carried out on a Renishaw inVia unit using the Ar ion laser with an excitation wavelength of 514.5 nm. The wide-angle X-ray diffraction pattern was conducted on a Bruker D8 Advance X-ray diffractometer with Cu K-alpha radiation. The diffraction data were collected in step scans, with a step size of 0.05° (2θ) and a count time of 2 s per step between 10 and 100° (2θ). X-ray photoelectron spectroscopic (XPS) measurements were performed on a Perkin Elmer PHI 5000C ESCA system with a monochromic Al K-alpha X-ray source. Before each analysis, the samples were dried under vacuum at 80°C. Spectra obtained over a scan range of 0–1100 eV were recorded and stored using the PHI ACCESS data system, and analyzed with XPSPEAK41 software.

Electrochemical measurements were conducted on a computer-controlled electrochemical workstation (Autolab PGSTAT 302N) with a typical three-electrode cell equipped with gas flow systems. A glassy carbon (GC) disk electrode (3 mm in diameter, Pine Research Instrumentation) coated with I-NG (I-NG/GC), NG (NG/GC), mpg-C₃N₄ (mpg-C₃N₄/GC) or Pt/C (20% of Pt/C, BASF; Pt/C/GC) was used as working electrode, an Ag/AgCl electrode (3 M KCl-filled) as reference electrode, and a platinum wire as counter electrode. An aqueous solution of 50 mM PBS (pH 7.0), which was prepared by mixing the stock solution of Na₂HPO₄ and NaH₂PO₄, was applied as the electrolyte for voltammogram measurements. Cyclic voltammogram (CV) measurements were carried out to characterize electrochemical activities on the electrode surface by measuring the current response on electrode surface to a specific range of potentials with a scan rate of 0.1 V s⁻¹. Rotating ring-disk electrode (RRDE) voltammogram measurements were prepared on a GC ring-disk electrode (5 mm diameter glassy carbon core and 9 mm outer diameter, Pine Research Instrumentation). During the preparation of working electrode, the GC was successively polished using 1.0 and 0.3 µm alumina powder followed by rinsing thoroughly with doubly distilled water. After successive sonication in 1 : 1 nitric acid, acetone, and doubly distilled water, the electrode was rinsed and dried at room temperature. A 5 µL 4 mg/mL of catalyst suspension was dropped on the surface of the pretreated GC (or 2.5 µL 2 mg/mL of catalyst suspension was dropped on the GC disk part for RRDE measurement) and dried under vacuum to obtain the working electrode. Before the RRDE measurements, oxygen gas was saturated in the electrolyte by bubbling the gas for 30 min. All electrochemical experiments (except as noted) were carried out at room temperature.

The internal resistance (R_{in}) of MFCs was determined by electrochemical impedance spectroscopy (EIS) according to the method described by Bard and Faulkner[40]. Impedance measurements were carried out at open circuit voltage (OCV) in a frequency range of 0.05 to 10⁵ Hz with sinusoidal perturbation amplitude of 10 mV. After the power in MFCs was generated stably, the external resistance (R_{ext}) was in turn shifted in the range of 10 to 10⁴ Ω to prepare the polarization and power curves. At each resistance, MFCs were operated for at least three batches to ensure the repeatable voltage output.

MFC configuration and operation. The electrochemical reactors used in this study were membrane-free single-chamber air-cathode MFCs constructed as previously reported[41]. The anodes were carbon fiber brushes that had a two-wire Ti core as the current collector and treated by the method of Feng et al[42]. The cathodes were made of carbon cloth (30% wet proofed, BASF) containing a catalyst loading of 0.5 mg cm⁻² on the water-facing side, with four PTFE diffusion layers and one carbon base layer on the air-facing side. The cathode catalysts examined in the present study were the synthesized materials including I-NG and NG. In order to compare the performance of the synthesized catalysts with the commonly used cathode catalyst, MFCs with a commercial Pt catalyst (20% of Pt/C, BASF) were set as the reference test. A cathode containing only carbon powder (Vulcan XC-72) was prepared as a non-catalyst control to investigate the electrocatalytic durability of cathode catalysts in MFCs.

During the start-up of MFCs, all reactors were inoculated with suspended bacteria from an acetate-fed MFC reactor that had been operating for about 6 months, and filled with acetate-laden synthetic wastewater containing (1 L of 50 mM phosphate buffer solution, pH 7.0) NaAc (a preferred carbon source for exoelectrogenic bacteria[43,44], 1000 mg; NH₄Cl, 310 mg; KCl 130 mg; and minerals and vitamins as described by Lovely and Phillips[45]. As the voltage dropped below 20 mV, the feed solution in the MFC reactor was replaced to form one complete operation cycle. After the voltages generated in MFCs maintained stable, the inoculum was omitted from the solution and the experimental data were recorded. The external resistance was fixed at 1000 Ω (except as noted) and all reactors were operated in batch mode at room temperature.

Calculation. Voltages from MFCs were recorded with a multicoated voltage collection instrument (12-bit A/D-conversion chips US) connected to a personal computer via an universal serial bus (USB) interface and calibrated with a digital multimeter (Fluke 17B; Fluke, USA) before each test. Power density was calculated according to P (mW/m²) = $10E^2/(R_{ext}A)$, where the factor of 10 is needed for the given units, E (mV) is the voltage, R_{ext} (Ω) is the external resistance, and A (cm²) is the project surface area of the electrode in MFCs.

1. Harnisch, F. & Schröder, W. From MFC to MXC: chemical and biological cathodes and their potential for microbial bioelectrochemical systems. *Chem. Soc. Rev.* **39**, 4433–4448 (2010).
2. Greeley, J. et al. Alloys of platinum and early transition metals as oxygen reduction electrocatalysts. *Nat. Chem.* **1**, 552–556 (2009).
3. Georgakilas, V. et al. Functionalization of graphene: covalent and non-covalent approaches, derivatives and applications. *Chem. Rev.* **112**, 6516–6214 (2012).
4. Gong, K. P., Du, F., Xia, Z. H., Durstock, M. & Dai, L. M. Nitrogen-doped carbon nanotube arrays with high electrocatalytic activity for oxygen reduction. *Science* **323**, 760–764 (2009).
5. Sun, X. J. et al. A class of high performance metal-free oxygen reduction electrocatalysts based on cheap carbon blacks. *Sci Rep* **3**, 2505 (2013).
6. Jeon, I. Y. et al. Facile, scalable synthesis of edge-halogenated graphene nanoplatelets as efficient metal-free eletrocatalysts for oxygen reduction reaction. *Sci Rep* **3**, 1810 (2013).
7. Qu, L. T., Liu, Y., Baek, J. B. & Dai, L. M. Nitrogen-doped graphene as efficient metal-free electrocatalyst for oxygen reduction in fuel cells. *ACS Nano* **4**, 1321–1326 (2010).
8. Feng, L. Y., Chen, Y. G. & Chen, L. Easy-to-operate and low-temperature synthesis of gram-scale nitrogen-doped graphene and its application as cathode catalyst in microbial fuel cells. *ACS Nano* **4**, 9611–9618 (2011).
9. Zhao, Y. et al. A versatile, ultralight, nitrogen-doped graphene framework. *Angew. Chem. Int. Ed.* **51**, 11371–11375 (2012).
10. Li, Q. Q., Zhang, S., Dai, L. M. & Li, L. S. Nitrogen-doped colloidal graphene quantum dots and their size-dependent electrocatalytic activity for the oxygen reduction reaction. *J. Am. Chem. Soc.* **134**, 18932–18935 (2012).
11. Zheng, Y., Liu, J., Liang, J., Jaroniec, M. & Qiao, S. Z. Graphitic carbon nitride materials: controllable synthesis and applications in fuel cells and photocatalysis. *Energy Environ. Sci.* **5**, 6717–6731 (2012).
12. Zhao, Y., Watanabe, K. & Hashimoto, K. J. Self-supporting oxygen reduction electrocatalysts made from a nitrogen-rich network polymer. *J. Am. Chem. Soc.* **134**, 19528–19531 (2012).
13. Liang, J. et al. Facile oxygen reduction on a three-dimensionally ordered macroporous graphitic C3N4/carbon composite electrocatalyst. *Angew. Chem. Int. Ed.* **51**, 3892–3896 (2012).
14. Yang, S. B., Feng, X. L., Wang, X. C. & Müllen, K. Graphene-based carbon nitride nanosheets as efficient metal-free electrocatalysts for oxygen reduction reactions. *Angew. Chem. Int. Ed.* **50**, 5339–5343 (2011).
15. Zheng, Y. et al. Nanoporous graphitic-C3N4@carbon metal-free electrocatalysts for highly efficient oxygen reduction. *J. Am. Chem. Soc.* **133**, 20116–20119 (2011).

16. Yu, D. S. *et al.* Nitrogen doped holey graphene as an efficient metal-free multifunctional electrochemical catalyst for hydrazine oxidation and oxygen reduction. *Nanoscale* **5**, 3457–3464 (2013).

17. Logan, B. E. & Rabaey, K. Conversion of wastes into bioelectricity and chemicals by using microbial electrochemical technologies. *Science* **337**, 686–690 (2012).

18. Wei, D. C. *et al.* Synthesis of N-doped graphene by chemical vapor deposition and its electrical properties. *Nano Lett.* **9**, 1752–1758 (2009).

19. Zhang, C. *et al.* Synthesis of nitrogen-doped graphene using embedded carbon and nitrogen sources. *Adv. Mater.* **23**, 1020–1024 (2011).

20. Sun, Z. Z. *et al.* Growth of graphene from solid carbon sources. *Nature* **468**, 549–552 (2010).

21. Panchakarla, L. S. *et al.* Synthesis, structure, and properties of boron- and nitrogen-doped graphene. *Adv. Mater.* **21**, 4726–4730 (2009).

22. Wang, Y., Shao, Y. Y., Matson, D. W., Li, J. H. & Lin, Y. H. Nitrogen-doped graphene and its application in electrochemical biosensing. *ACS Nano* **4**, 1790–1798 (2010).

23. Collins, P. G., Bradley, K., Ishigami, M. & Zettl, A. Extreme oxygen sensitivity of electronic properties of carbon nanotubes. *Science* **287**, 1801–1804 (2000).

24. Logan, B. E. & Regan, J. M. Microbial fuel cells challenges and applications. *Environ. Sci. Technol.* **40**, 5172–5180 (2006).

25. Zhao, F. *et al.* Challenges and constraints of using oxygen cathodes in microbial fuel cells. *Environ. Sci. Technol.* **40**, 5193–5199 (2006).

26. Kundu, S. *et al.* Electrocatalytic Activity and Stability of Nitrogen-Containing Carbon Nanotubes in the Oxygen Reduction Reaction. *J. Phys. Chem. C* **113**, 14302–14310 (2009).

27. Rao, C. V., Cabrera, C. R. & Ishikawa, Y. In search of the active site in nitrogen-doped carbon nanotube electrodes for the oxygen reduction reaction. *J. Phys. Chem. Lett.* **1**, 2622–2627 (2010).

28. Lai, L. F. *et al.* Exploration of the active center structure of nitrogen-doped graphene-based catalysts for oxygen reduction reaction. *Energy Environ. Sci.* **5**, 7936–7942 (2012).

29. Bashyam, R. & Zelenay, P. A class of non-precious metal composite catalysts for fuel cells. *Nature* **443**, 63–66 (2006).

30. Liang, Y. Y. *et al.* Co_3O_4 nanocrystals on graphene as a synergistic catalyst for oxygen reduction reaction. *Nat. Mater.* **10**, 780–786 (2011).

31. Lefèvre, M., Proietti, E., Jaouen, F. & Dodelet, J. Iron-based catalysts with improved oxygen reduction activity in polymer electrolyte fuel cells. *Science* **324**, 71–74 (2009).

32. Cheng, S. A., Liu, H. & Logan, B. E. Power densities using different cathode catalysts (Pt and CoTMPP) and polymer binders (Nafion and PTFE) in single chamber microbial fuel cells. *Environ. Sci. Technol.* **40**, 364–369 (2006).

33. Chen, S. L. *et al.* Stainless steel mesh supported nitrogen-doped carbon nanofibers for binder-free cathode in microbial fuel cells. *Biosens. Bioelectron.* **34**, 282–285 (2012).

34. Renslow, R. *et al.* Oxygen reduction kinetics on graphite cathodes in sediment microbial fuel cells. *Phys. Chem. Chem. Phys.* **13**, 21573–21584 (2011).

35. Qiao, Y., Bao, S. J. & Li, C. M. Electrocatalysis in microbial fuel cells—from electrode material to direct electrochemistry. *Energy Environ. Sci.* **3**, 544–553 (2010).

36. Wang, H. B., Maiyalagan, T. & Wang, X. Review on recent progress in nitrogen-doped graphene: synthesis, characterization, and its potential applications. *ACS Catal.* **2**, 781–794 (2012).

37. Yang, S. B., Feng, X. L. & Müllen, K. Sandwich-like, graphene-based titania nanosheets with high surface area for fast lithium storage. *Adv. Mater.* **23**, 3575–3579 (2011).

38. Yang, S. B. *et al.* Graphene-based nanosheets with a sandwich structure. *Angew. Chem., Int. Ed.* **49**, 4795–4799 (2010).

39. Goettmann, F., Fischer, A., Antonietti, M. & Thomas, A. Chemical synthesis of mesoporous carbon nitrides using hard templates and their use as a metal-free catalyst for friedel–crafts reaction of benzene. *Angew. Chem., Int. Ed.* **45**, 4467–4471 (2006).

40. Bard, A. J. & Faulkner, L. R. *Electrochemical methods: fundamentals and applications 2nd Edition.* pp 383–388 (John Willey & Sons, New York, 2001).

41. Logan, B. E., Cheng, S. A., Watson, V. & Estadt, G. Graphite fiber brush anodes for increased power production in air-cathode microbial fuel cells. *Environ. Sci. Technol.* **41**, 3341–3346 (2007).

42. Feng, Y. J., Yang, Q., Wang, X. & Logan, B. E. Treatment of carbon fiber brush anodes for improving power generation in air–cathode microbial fuel cells. *J. Power Sources* **195**, 1841–1844 (2010).

43. Logan, B. E. & Rabaey, K. Conversion of wastes into bioelectricity and chemicals by using microbial electrochemical technologies. *Science* **337**, 686–690 (2012).

44. Logan, B. E. & Elimelech, M. Membrane-based processes for sustainable power generation using water. *Nature* **488**, 313–319 (2012).

45. Lovley, D. R. & Phillips, E. J. P. Novel mode of microbial energy metabolism: organic carbon oxidation coupled to dissimilatory reduction of iron or manganese. *Appl. Environ. Microbiol.* **54**, 1472–1480 (1998).

Acknowledgments

Author contributions

L.F. and J.L. conceived the study design and co-wrote the paper. J.L. and L.Y. performed the synthesis and morphological and structural characterization. L.F. and L.Y. contributed to electrocatalytic activity evaluation. Z.H., M.L. and D.W. performed the operation of MFC reactors. Y.C. supervised the project. All authors contributed to the scientific planning and discussions.

Additional information